www.czasopisma.pan.pl www.journals.pan.pl

BULLETIN OF THE POLISH ACADEMY OF SCIENCES
TECHNICAL SCIENCES, Vol. 66, No. 2, 2018
DOI: 10.24425/122102

Analysis of selected properties of asphalt concrete with synthetic wax

G. MAZUREK* and M. IWAŃSKI

Department of Transportation Engineering, Kielce University of Technology

Abstract. This article discusses the issue of viscoplastic deformation that usually occurs in road pavements, especially in the summer season in Poland. The evaluation of viscoplastic deformations was performed on the example of the asphalt concrete designated for the binding course layer (AC16W). Additionally, the bitumen used for manufacturing asphalt concrete samples was modified with two types of synthetic waxes widely applied in the warm mix asphalt technology. These waxes varied in molecular weight, which affected their softening point results. Before decomposition of the total strain into elastic and viscoplastic part, oscillatory tests in the linear viscoelastic region were required. The generalized Maxwell model was used to describe the behavior of asphalt concrete in the linear viscoelastic range. Using the elasto-viscoelastic correspondence principle, described by Schapery, the initial yield strength stress was evaluated. The pseudostrain variable turned out to be useful for estimating the onset of viscoplastic strains occurring in road pavement. Such engineering procedure approach could result in faster approximation of the yield strength level during the design of pavement structures. It will also allow for differentiation of mixtures in terms of their susceptibility to permanent deformation and of their sensitivity to traffic induced overloading.

Key words: initial yield strength, synthetic wax, Prony Series, pseudostrains, viscoplastic deformation.

1. Introduction

Viscoplastic deformations are one of the major distress types that occur in the structure of road pavements. The source of their formation in Poland is the permanent deformation due to excessive shear stresses generated by heavy vehicles during hot summer months. The total viscoplastic deformation of the pavement layer system is equal to the sum of the deformations in individual pavement layers [1]. Taking into account their high stiffness, as compared with that of the subgrade [2, 34], the contribution of the bituminous layers susceptibility to the overall deformation of the pavement structure will be significant. Viscoplastic deformation results from the displacement of aggregate grains in asphalt concrete coupled with the viscous flow of bitumen caused by high bitumen temperatures [3]. Experimental studies confirm the assumption that rut formation results from a combination of AC densification and shear deformations, and occurs especially at the wheel-pavement contact surface where shear stress prevails considerably over the stresses of lateral confinement [4]. This process, however understandable, is difficult to model [5].

An important rutting prevention issue in asphalt mixture design is the use of increased viscosity binders without significantly altering their flexibility at low temperatures. Therefore, warm mix asphalt [11, 12] and half-warm mix asphalt [32] technologies are becoming increasingly popular. In order to bring bitumen viscosity below the reference temperature set for asphalt mixtures with bitumen 35/50 [14] as the equivalent of 140°C, modern synthetic waxes or foaming processes are used. Synthetic waxes increase zero shear viscosity and stiffness of the base bitumen [29], and the yield strength is induced by fine crystallites of the wax [33]. Proper modeling of elasto-viscoplastic behavior of such synthetic wax-modified asphalt mixtures requires the application of models based on the viscoelasticity theory [6, 35]. Depending on the nature of bitumen modification, asphalt concrete layers achieve different levels of viscoplastic deformation, depending on the induced strain rate and temperature [36]. After an initial compaction period, the permanent deformation per wheel pass is proportional to the static axle load and inversely proportional to the vehicle speed [37]. Viscoplastic state of these mixtures can be described by a number of models. For steel, the yield surface model, dependent exclusively on the combination of shear stresses such as those described by the Von-Mises theory, can be used. In the case of asphalt mixtures, the yield surface must take into account the behavior typical for geomaterials whose strength depends on the state of lateral confinement. Realistic plastic flow limit description, accounting for the internal friction of aggregates and cohesion, is provided by Mohr-Coulomb or Drucker-Prager models.

In engineering practice, it is extremely important to define the correct yield strength at which viscoplastic deformation begins [7]. In materials such as steel, which are subject to elastic theory [18], the transition from linear to non-linear stress-strain ratio is not difficult to determine. In contrast, in elastic-viscoplastic materials – such as asphalt concrete – it is not possible to locate the apparent stress-strain relationship on the basis of the $\sigma = f(\varepsilon)$ formula. Even a small level of stress applied to a specimen of asphalt concrete will in a short time cause non-linearity in the stress-strain relationship, caused by the immediate relaxation of the stress. It should be added that

*e-mail: gmazurek@tu.kielce.pl

Manuscript submitted 2017-08-21, revised 2017-11-14, initially accepted for publication 2018-01-20, published in April 2018.

in Poland a linear elastic model at an equivalent temperature of 13°C [38] is commonly adopted for the road structure design. It does not define the boundary conditions of the stress causing permanent deformations. Lack of a clear yield threshold, confirmed by many researchers already [8, 9], affects the behavior of asphalt mixtures at stresses close to yield surface [39]. In order to determine the beginning of asphalt concrete flow (required in the Drucker-Prager model), the total stress has to be decomposed to reduce the viscoelastic behavior tolerations based on elasticity equations, which make use of pseudostrain rather than strain values. Viscoelasticity theory can be used to determine the stress state which when passed leads to visco-plastic damage and microcracks in the asphalt mixture. This description is offered by the VEPCD model (viscoelastoplastic continuum damage model), integrating two types of equations resulting from the theory of elasticity with pseudostrains, and the strain-hardening model based on the Work Potential Theory [10]. A relatively quick evaluation of the yield strength allows a more accurate assessment of the sensitivity of asphalt concrete and other asphalt mixtures to shear stress levels. With the assumption that the material is isotropic and with some approximation, the compressive yield stress level can be used for FE modeling of pavement stress and strain states. This article focuses on the phase between the end of the linear elastic behavior of asphalt concrete and the state of ideal plasticity as determined by the Mohr-Coulomb model (M-C). It should be noted that as a result of the relaxation phenomenon there is no instantaneous transition to the yielding state in the asphalt concrete, and this is accompanied by gradual increase in visco-elastic deformation whose rate depends on the temperature and strain rate of the asphalt concrete [40]. Due to the preliminary nature of this research, the article did not take into account the scope of modeling asphalt concrete behavior after exceeding the initial yield limit stress.

2. Materials and procedures

2.1. Bitumen and modifiers. Two types of synthetic wax derived from the Fisher-Tropsch synthesis were used in the study [11, 12]. The waxes varied in molecular weight and the resulting

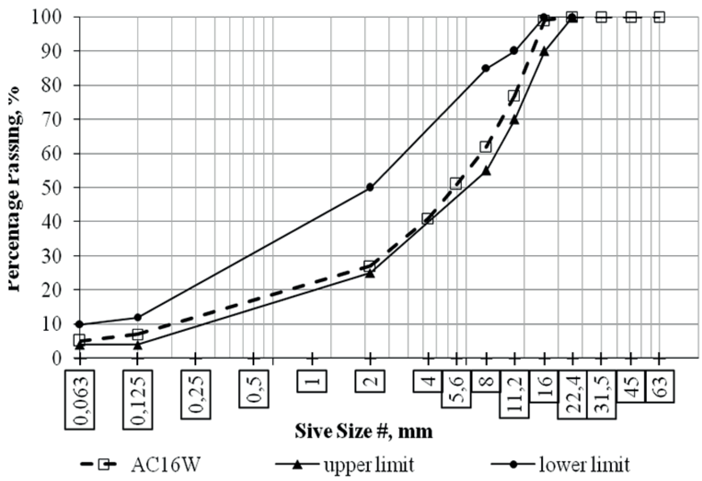

Fig. 1. Particle size distribution of AC16W

softening point. The lower molecular weight (lower density) synthetic wax was designated as "M", while the one with the higher molecular weight was designated as "N". Input bitumen 35/50 was marked with a "Z". Basic rheological properties of the synthetic waxes, as declared in the product sheets, are presented in Table 1.

As the wax present in the bitumen can be treated as a fine-crystalline filler below its softening point [13], one should expect an increase in the yield strength of the bitumen and, hence, of the asphalt concrete.

2.2. Mineral mix design. The AC16W mixture met the requirements set out in the Polish guidelines WT-2/2010 [14] for the pavement layer subject to the KR3-6 design traffic load ($ESAL_{100\,kN} < 2.5 \cdot 10^6 \div 7.3 \cdot 10^6$ axles). The AC16W mineral mix composition was designed using the limit curve method, with the critical values following the WT-2/2010 requirements. Figure 1 shows the grading curve of the AC16W mixture.

Limestone fractions 8/16 and 2/8 mm and dolomite 0/4 mm were used as aggregates in the AC16W mix. Proper adhesion between the bitumen and aggregate was ensured by incorporation of a 0.1% adhesion agent.

Table 1
Basic rheological parameters of synthetic waxes and of modified bitumen 35/50

Parameter	u.m.	Value				
		Synthetic wax type M (soft wax)	Synthetic wax type N (hard wax)	Bitumen 35/50 Z	Bitumen 35/50 + 2.5% M	Bitumen 35/50 + 2.5% N
Softening temperature	°C	81	100	52	68	75
Penetration	0.1 mm	9	<1	41	28	35
Flash point	°C	>200	>285	>240	–	–
Kinematic viscosity at 135°C	cSt	9	12	6	4	3
Density at 25°C	Mg/m^3	0.9	0.94	0.99	–	–

Table 2
Basic physical and mechanical properties of AC16W

Parameter	Mixture type			Criterion	Standard
	AC16W-Z	AC16W-M	AC16-N		
Volumetric density ρ_{ssd}, Mg/m^3	2.347	2.346	2.347	–	PN-EN 12697–6
AC mix air void content V_m, % (v/v)	5.7	6.5	6.2	4.0 ÷ 7.0	PN-EN 12697–8
Filling the void space with bitumen VFB, %	65.11	62.03	63.14	–	PN-EN 12697–8
Mineral mix air void content mm, % (v/v)	16.34	17.01	16.74	–	PN-EN 12697–8
Thickening temperature, °C	145	130	130	–	–

2.3. Basic physical and mechanical properties of the AC16W layer. The optimum bitumen content in all the mixtures was decided at 4.6%, established for the reference mixture (AC16W-Z) by means of the Marshall test. The bitumen was modified with 2.5% of M and N waxes at 155°C for 30 minutes at the blender speed of 400 rev/min. The modified bitumen was used to make four AC specimens for each modification variant. A total of 12 AC16W specimens were thus prepared. The specimens were compacted in the gyratory press to adjust their dimensions to the requirements of the stiffness modulus test procedure, DTC-CY (PN-EN 12697–26 Annex D) [15] and NCHRP Report 614 [16]. Table 2 outlines the basic physical and mechanical properties of the asphalt concrete determined during the tests.

The primary aim was to obtain comparable compaction values in asphalt concrete specimens. The non-parametric Kruskal-Wallis test (ANOVA) performed for all the specimens revealed that at significance level $\alpha = 0.05$, the air void content differences due to the type of synthetic wax used were not statistically significant (p-value = 0.1561).

2.4. Complex modulus in the linear viscoelastic range. The complex modulus of AC16W was determined by means of the Direct Tension-Compression Test on Cylindrical Specimens (DTC-CY) in accordance with PN-EN 12697–26, Annex D. Four replicates of 101 mm in diameter were prepared for each case under investigation, where the diameter was more than four times the maximum size of the grain in the mixture. The specimen height (H) to diameter (D) ratio was 1.8. The specimen was subjected to a steady sinusoidal strain with amplitude $\varepsilon_0 < 25\mu\varepsilon$. The complex modulus was determined at 10°C, 20°C and 40°C. The load frequency was 0.1 Hz, 0.3 Hz, 1 Hz, 3 Hz, 10 Hz and 20 Hz. The data produced from the tests included complex modulus (E*) and phase angle (δ).

2.5. Axial shear in strain control. The same specimens were used first in the non-destructive stiffness modulus test and then in the axial compression test. The range of applied strain in the linear viscoelasticity should not cause energy dissipation, i.e. the stiffness modulus test was performed without distorting the asphalt concrete structure. The test was designed in accordance with the ASTM D 2166 procedure [17] supplemented with the researchers' experience [2]. The monotonic strain pattern for velocity $\varepsilon = 333 {}^{\mu\varepsilon}/_{S}$. was used. This strain rate was adopted to minimize the impact of creep in the asphalt concrete. The test temperature was 40°C, representing the average temperature conditions in the pavement during the summer season.

3. Viscoelastic properties of asphalt concrete

Prediction of viscoelastic properties can be made using many rheological and mathematical models. Using them, it was possible to build master curves describing the behavior of the mineral-asphalt mixture throughout a wide range of temperatures and loading times. The most popular models are: the Burgers model [41], the modified Huet-Sayegh (2S2P1D) [22] and the generalized Maxwell model. The 2S2P1D and generalized Maxwell model can be used for master curves construction. In the case of the Burgers model, its application in such form is troublesome. This is due to the fact that the rheological parameters incorporated into this model are temperature dependent and the classical horizontal linear shift factor cannot be applied. Also in work [42] it has been found that it could be applicable for constant temperature and small frequency range. Based on comparative studies [47] in the LVE range, the Burgers model at low frequencies yields significantly different results for relaxation modulus (|E*| also denotes a dynamic modulus) than other models. It should be added that the greatest similarity was obtained between the 2S2P1D model and the generalized Maxwell model in the frequency range from 0.1 to 10 Hz. Similar conclusions were obtained in paper [43]. The quality of matching experimental to modeled results stated that the generalized Maxwell model depends on the number of individual simple Maxwell networks. This way, it is possible to explain some singularities in the results of dynamic modulus losing the final model generalization degree. Nevertheless, in Woldekidan's work [44] a generalized Maxwell model was used to describe the behavior of bitumen and asphalt mastics, as recommended. According to some authors [22, 42], using the fractional model is the most rational choice from the point of view of the Cole-Cole diagram. Nevertheless, easy transformation of the asphalt concrete description in the LVE range for the generalized Maxwell model from the time domain to the frequency domain and then of the 2SP1D model [10, 44], and its application in the VEPCD model resulted in the generalized Maxwell model being selected for further analysis.

The first stage of testing was the most important part of the experiment. It aimed at defining a set of rheological parameters of the generalized Maxwell model (or the Wiechert model) in the linear viscoelastic range (LVE). Accuracy in estimating rheological parameters for asphalt concrete using this model will have a substantial effect on the accuracy of determining AC viscoplastic strains. Viscoplastic strain is determined through the decomposition of the total strain, as suggested by Schapery [19], into viscoelastic (ε_{ve}) and viscoplastic (ε_{vp}) strain components. Details of the decomposition approach will be discussed further in the article. In the first step, a non-destructive measurement technique has to be used to determine the instantaneous stiffness modulus $E_o(t \to 0)$. The test methods for measuring the parameters of the relaxation function in the generalized Maxwell model (GM) include the static creep test and dynamic test with oscillatory loading in strain control, in accordance with PN-EN 12697–26, Annex D. The latter type of testing is more suitable when the instantaneous stiffness modulus E_o is to be found. As the static creep test does not allow immediate loading of specimens, dynamic testing was chosen for the experiment.

Parameters of the GM model (Prony Series) can be obtained from the imaginary component (E″) and real component (E′) of the complex modulus (E*) in the frequency domain, using the Fourier transform. The complex modulus E* [20] is expressed by:

$$E^* = E' + iE''. \tag{1}$$

Where: E′ is the real component of the complex modulus and E″ is the imaginary component of the complex modulus. Formulas (2) and (3) represent E* components

$$E' = E_o - \sum_{i=1}^{N} E_i + \sum_{i=1}^{N} \frac{E_i \cdot \tau_i^2 \cdot \varpi^2}{1 + \tau_i^2 \cdot \varpi^2} \tag{2}$$

$$E'' = \sum_{i=1}^{N} \frac{E_i \cdot \tau_i \cdot \varpi}{1 + \tau_i^2 \cdot \varpi^2}. \tag{3}$$

Where: E_i is the ith elastic modulus in the GM, E_o is the instantaneous elastic modulus, τ_i is the ith relaxation time in the GM, and ω_i is the reduced frequency. Non-linear least squares estimation of the model parameters was used and the objective function was minimized at the set initial values. A flow script was prepared in Mathcad for finding a minimum of the objective function, implemented using the Quasi-Newton method. Three test temperatures were used (10°C, 20°C and 40°C) and the time-temperature superposition principle (TTSP), which links loading frequency and temperature into a temperature shift factor α_T, was applied to construct the master curve of the modulus [21]. The equation used has the following form (4):

$$\alpha^T = \omega \cdot e^{(A_1 + T \cdot A_2)}. \tag{4}$$

Where: T – test temperature, ω – frequency at test temperature, A_1, A_2 – parameters of the model. The quality of fit of the model

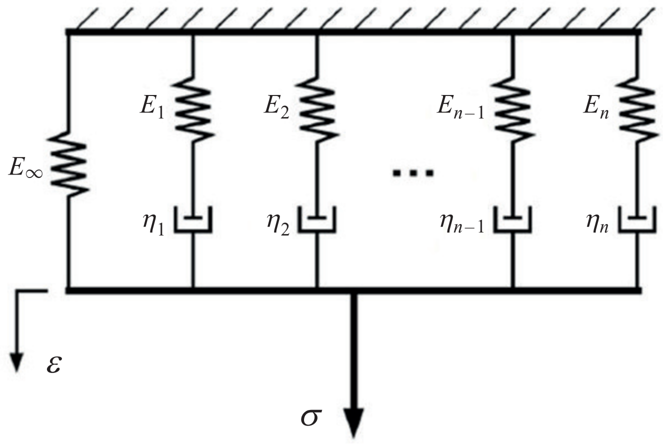

Fig. 2. Graphical illustration of the generalized Maxwell model [45]

to the experimental data was determined by two qualitative measures, the determination coefficient R^2 and mean normalized error (MNE) [22]. As during the destructive axial compressive testing of asphalt concrete the monotonically applied strain was time-controlled, the results of the master curve at the reference temperature of 40°C also had to be presented as a function of time, with Fourier transforms employed. The master curve was plotted from formula (5):

$$E(t) = E_\infty + \left[\sum_{i=1}^{n} E_i \cdot \left[e^{\left(\frac{t}{\tau_i}\right)}\right]\right]. \tag{5}$$

Where: E_∞ – long-term equilibrium stiffness modulus at $t \to \infty$ ($E_\infty = E_o - \sum_{i=1}^{n} E_i$), E_o – instantaneous stiffness modulus at $t \to 0$, E_i – ith stiffness modulus of the GM, τ_i – relaxation time, t – the reduced loading time.

The above formula of the asphalt concrete relaxation function was illustrated as an assembly of springs and dashpots (Fig. 2).

As a result of the transformations, the value of the reference stiffness modulus E_R, equivalent to the instantaneous stiffness modulus E_o, can be determined with greater accuracy (greater than in static creep tests). The value of the reference stiffness modulus is necessary to determine the value of pseudostrains ε_R.

4. Initial yield strength of asphalt concrete

The initial yield strength σ_{pl} is the value of the stress at which non-reversible viscoplastic deformation begins. It cannot be determined for viscoelastic materials, such as asphalt mixtures, where at high temperatures the viscous component of the strain is significant. As the load time will noticeably affect the stress relaxation rate, it will not be possible to find the linear $\sigma - \varepsilon$ relationship. However, even though the strain rate in the asphalt concrete specimen is linear, this change in stress will be nonlinear. The time-dependent change in stress is described by formula (6) [1]:

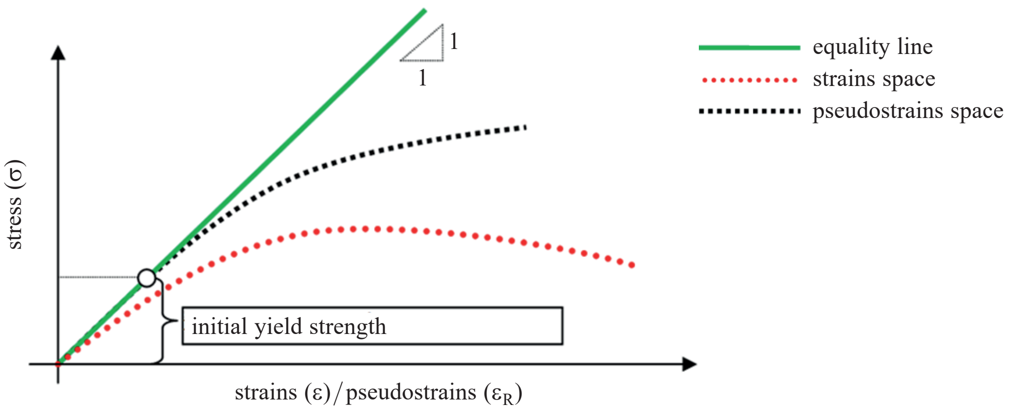

Fig. 3. Stress-strain (pseudostrain) behavior of asphalt concrete in strain-controlled-rate monotonic test

$$\sigma(t) = \int_o^t E(t-\tau) \cdot \frac{\partial \varepsilon}{\partial \tau} \cdot d\tau. \tag{6}$$

Where: $\sigma(t)$ – stress as a function of the reduced time, $\frac{\partial \varepsilon}{\partial \tau}$ – strain rate, $d\tau$ – integration constant, t – reduced time. In order to determine the beginning of the asphalt concrete mix flow, it is necessary to use the pseudostrain variable ε_R. It is based on the elasto-viscoelastic correspondence principle, as described by Schapery. This is a form of simplification relating to the nonlinear effect in the $\sigma - \varepsilon$ relationship, resulting from the time-dependent stiffness change due to stress relaxation, and to the linear $\sigma - \varepsilon_R$ relationship [23]. The graphical interpretation of the discussed transformation is shown in Fig. 3, which presents the result of normalizing the actual strains to the new pseudostrain variable.

This will transform the time effect, inducing the non-linear change in the stiffness modulus of the viscoelastic material to the form of an elastic model as for elastic materials such as steel. Accordingly, the linear viscoelasticity relationship $\sigma - \varepsilon_R$ will be represented by a straight line in the graph, corresponding to the slope that can be obtained for the instantaneous stiffness modulus determined in oscillation tests. As a result, relationship $\sigma - \varepsilon_R$ has the following form (7):

$$\sigma = I \cdot \varepsilon_R \tag{7}$$

where: σ – stress, ε_R – pseudostrain, with reference value in the interval: 0.9 to 1.1. Equations (6) can be developed into the sum of partial strain relaxation functions depending on the variable rate of strain increment. With convolution (6), when $\frac{\partial \varepsilon}{\partial \tau} = \text{const.}$, the ultimate form of the pseudostrain function adopted in the experiment has the following form (8):

$$\varepsilon_R(t) = \frac{\partial \dot{\varepsilon}}{\varepsilon_R} \cdot \left[E_\infty \cdot t + \sum_{i=1}^n E_i \cdot \tau_i \cdot \left(1 - e^{\frac{t}{\tau_i}}\right)\right]. \tag{8}$$

Where $\dot{\varepsilon}$ – the rate of strain increment $\left(333^{\mu\varepsilon}/_S\right)$, E_R – the reference stiffness modulus equal to the instantaneous stiffness modulus. The main reason for using the pseudostrain variable instead of strain is that pseudostrains represent the total strain value ε^{Total} after subtracting from it only the viscous strain component ε_{vi} [9]. Accordingly, in the absence of viscoplasticstrains ε_{vp}, pseudostrains ε_R history is linear. Where ε_R deviates from the reference line, viscoplastic strains ε_{vp} occur, defined as (9):

$$\varepsilon_{vp} = \varepsilon_R\left(= \varepsilon^{Total} - \varepsilon_{vi}\right) - \varepsilon_e. \tag{9}$$

Where: ε_e – elastic strain $\left(^{\sigma}/_{E_o}\right)$, σ – stress ranging from σ_{pl} to its destructive value. With this simple method, the stress level σ_{pl}, at which a significant increase in viscoplastic deformation occurs, can be quickly identified. It is defined as the deviation of the $\sigma - \varepsilon_R$ relation from the reference line inclined relative to the ε_R axis of the graph at 45°. Knowledge of the initial yield strength σ_{pl} can be used for engineering purposes in the modeling of more complex stress states in which average deformation will be related to the stress initiating permanent viscoplastic deformation.

5. Test results

5.1. Viscoelastic parameters in the generalized Maxwell model in the LVE range. The first stage of the study required that the GM model parameters for linear viscoelasticity (LVE) be determined. The range of controlled strains 25µε ensured that the stiffness modulus was tested without any energy dissipation. The tests were carried out in accordance with PN-EN 12697–26, Annex D. The viscoelastic behavior of asphalt concrete AC16W was described with a maximum of six Maxwell elements connected in series on the basis of stiffness modulus and phase angle results. Increasing the number of elements did not significantly improve the fit of the model to the experimental data. Knowing that asphalt concrete in a range of small strains is a thermorheologically simple material [24], the load time and temperature were converted to a single master curve of the stiffness modulus via horizontal shifting [22]. The final form of the master curve comprised optimization with respect to the real and imaginary components of the stiffness modulus. Table 3 is a summary of the fitted GM parameters of the master curve.

Table 3
Master curve parameters of AC 16W on the basis of the Generalized Maxwell Model (GM)

Asphalt concrete AC 16W-Z (reference AC, with bitumen non-modified with synthetic wax)				
	Generalized Maxwell model parameters		Factor α_T (exponential function)	
	g_i [–]	τ_i [s]	A_1	A_2
Generalized Maxwell model (GM) parameters	$g_1 = 0.516$ $g_2 = 0.102$ $g_3 = 0.098$ $g_4 = 0.098$ $g_5 = 0.098$ $g_6 = 0.088$	$\tau_1 = 0$ $\tau_2 = 0.00008$ $\tau_3 = 0.00008$ $\tau_4 = 0.02812$ $\tau_5 = 0.02903$ $\tau_6 = 2.73278$	14.653	–0.320
	$E_o = 18600.75$MPa			
	$R^2 = 0.97$; RMSE = 11.7%			
Asphalt concrete AC 16W-M (with bitumen modified with 2.5% type M synthetic wax)				
	Generalized Maxwell model parameters		Factor α_T (exponential function)	
	g_i [–]	τ_i [s]	A_1	A_2
Generalized Maxwell model (GM) parameters	$g_1 = 0.317$ $g_2 = 0.317$ $g_3 = 0.183$ $g_4 = 0.183$ $g_5 = 1 \cdot 10^{-7}$	$\tau_1 = 0.00002$ $\tau_2 = 0.00064$ $\tau_3 = 0.02355$ $\tau_4 = 1.51353$ $\tau_5 = 1.51353$	12.27	–0.267
	$E_o = 22354.29$ MPa			
	$R^2 = 0.98$; RMSE = 8.6%			
Asphalt concrete AC 16W-N (with bitumen modified with 2.5% type N synthetic wax)				
	Generalized Maxwell model parameters		Factor α_T (exponential function)	
	g_i [–]	τ_i [s]	A_1	A_2
Generalized Maxwell model (GM) parameters	$g_1 = 0.280$ $g_2 = 0.247$ $g_3 = 0.184$ $g_4 = 0.1184$ $g_5 = 0.105$	$\tau_1 = 0.00004$ $\tau_2 = 0.00055$ $\tau_3 = 0.0056$ $\tau_4 = 0.06743$ $\tau_5 = 1.81881$	10.87	–0.267
	$E_o = 20650.07$ MPa			
	$R^2 = 0.99$; RMSE = 10.7%			

The results summarized in Table 3 indicate that fitting the model to the experimental data was performed with a moderate mean square error of less than 12%. The correlation coefficient was greater than 0.97. The largest scattering of the results, as indicated by mean squared error RMSE, was recorded for AC16W-Z. Nonetheless, all the fit quality results of the master curve model were considered satisfactory. The quality of fit in terms of the viscoelastic behavior of asphalt concrete, taking into account both the complex stiffness modulus and the phase angle, represents the Black curve well. Graphical representation of the Black curve is shown in Fig. 4. The unmodified AC mixtures had the lowest instantaneous stiffness modulus, i.e. $E_o = 18600.75$ MPa. The remaining two AC variants with synthetic wax had a higher instantaneous stiffness level and this was due to the action of synthetic wax crystallites in the bitumen. Note that the parameters of the temperature shift factor model are similar, so that the observed proportions in the readings of stiffness moduli at subsequent test temperatures are similar. The complex stiffness modulus, as mentioned earlier, was measured by forced oscillation, primarily to accurately evaluate the instantaneous stiffness modulus. The master curves of the stiffness modulus as a function of frequency were constructed based on the data in Table 3. For further analysis, it is necessary to present the stiffness modulus as a function of time. The results of the relaxation function in the frequency domain can be presented as a function of time using the relationships shown in formula (5). Graphical interpretation of the stiffness modulus master curves at 40°C adopted as the reference temperature in the analysis, is shown in Fig. 5.

The graphs in Fig. 5 show the highest stiffness in AC16W-M, i.e. asphalt concrete with type M synthetic wax

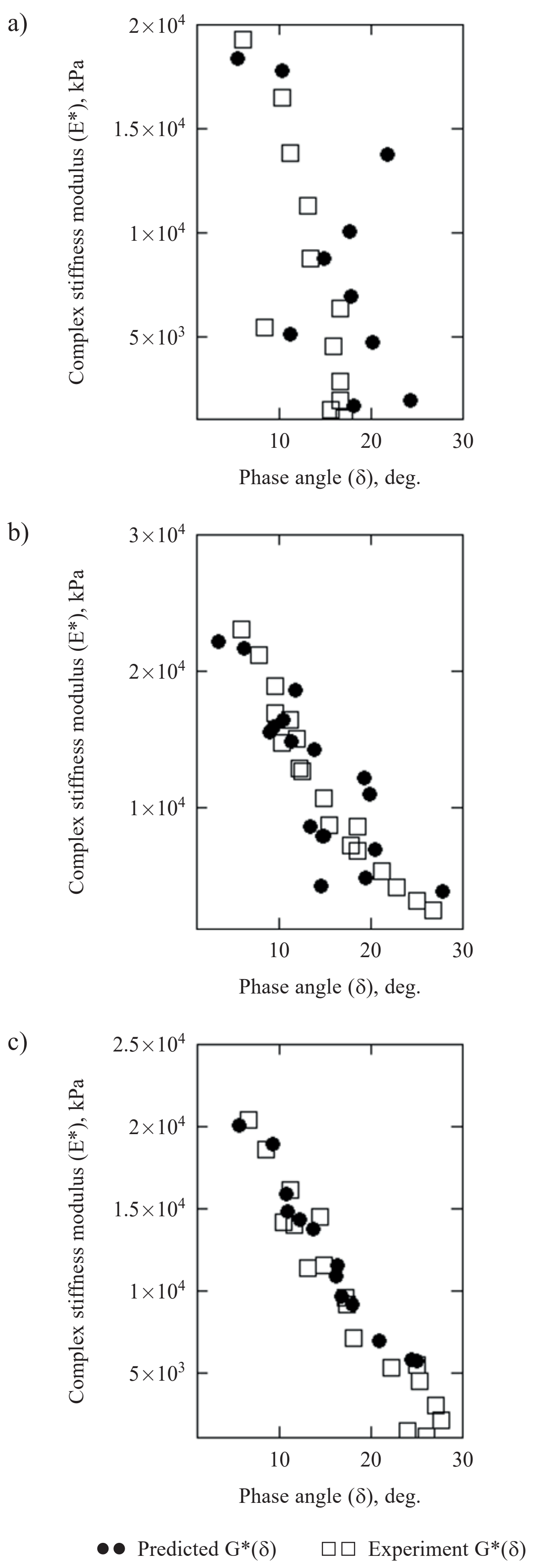

Fig. 4. Black curve at 40°C: a) AC16W-Z; b) AC16W-M; c) AC16W-N

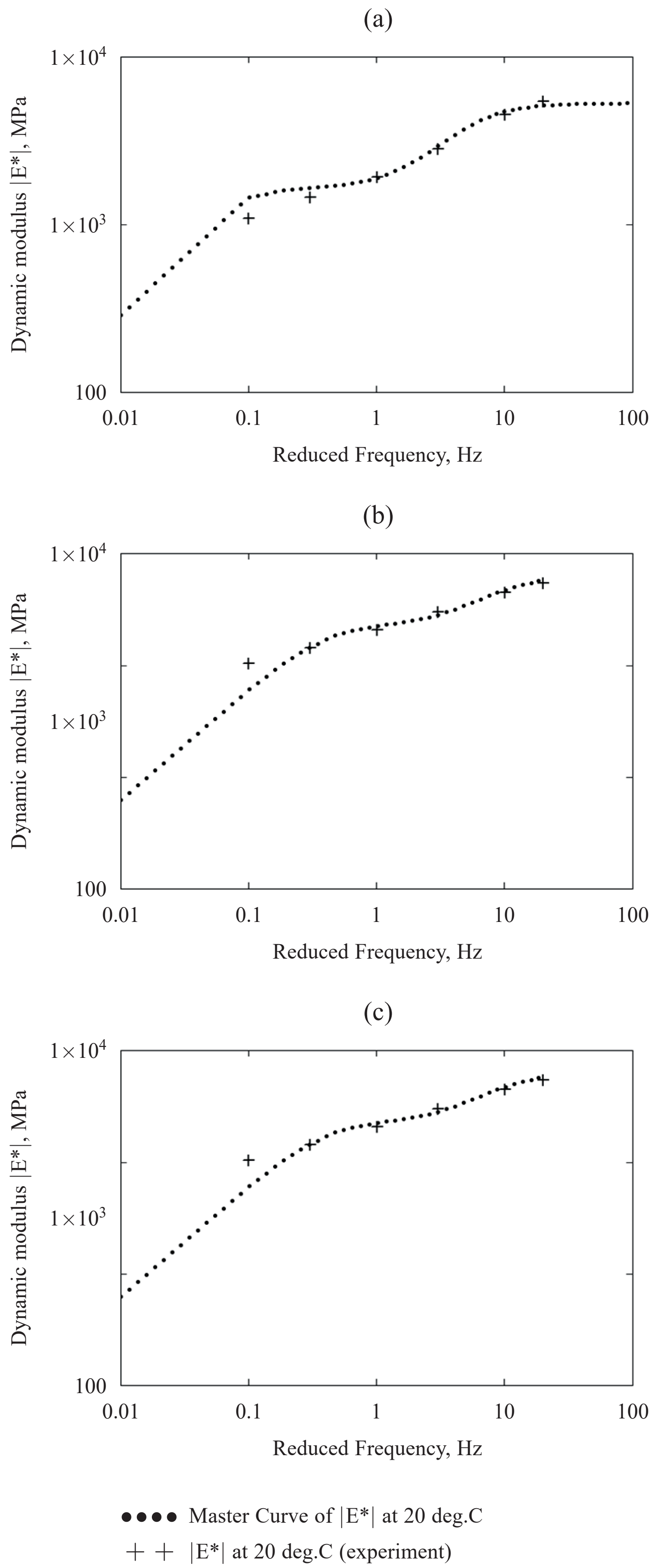

Fig. 5. Master curves of the stiffness modulus of asphalt concrete at 40°C: a) AC11W-Z; b) AC11W-M; c) AC11W-N

added. The AC containing type N hard wax (AC16W-N) showed the lowest stiffness. According to Table 3, at high frequency/short load time all the asphalt concrete specimens tend to follow an asymptotic level of instantaneous modulus (glassy modulus) in the range between 18600.75 and 22354.29 MPa. For long-term load time, asphalt concretes AC16W-Z and AC16W-M had similar values. At high frequencies, the reference asphalt concrete AC16W-Z had results comparable to those of AC16W-N. It is expected that at the standard load time, i.e. f = 10 Hz, assumed for designing new road pavements as required by Polish catalogue [25], asphalt concretes AC16W-M and AC16W-N will reduce the horizontal deformation at the bottom of asphalt concrete layers. Asphalt concrete AC16W-Z had a slightly lower dynamic modulus (at 10 Hz). These results refer to the state of the material in which there is no damage or micro damage in the structure of asphalt concrete [26]. The observed waveform of the relaxation function is related to the fact that the model consists of 5 to 6 Maxwell networks which are essentially a sum of simple sigmoid-like functions. Their catenation caused an increase in the fit of the experimental data to the modeled data. In the case of an infinite number of Maxwell networks, the form of the dynamic master curve in the frequency function will have a shape similar to the sigmoid function.

In conclusion, the behavior of the material in the LVE range determines its stiffness at very small strains. In Poland, however, pavement surfaces are exposed to multiple high strains at temperatures reaching 60°C. Accordingly, further analysis will focus on the material's response to high strain levels.

5.2. Determining the initial yield strength. The tests aimed at determining the stress level initiating viscoelastic deformation were performed in the axial compression mode for large strains exceeding the LVE range. Bearing in mind that the initial yield stress (the octahedral tangent stress) is directly proportional to the shear stress, it indicates the approximate moment when viscoplastic strain appears in the assumed state of compression stresses [27]. This classic relationship, which uses the second stress invariant, may also be related to a road surface [28].

The initial yield point determined in the uniaxial compression test can be highly important particularly in the contact area between the vehicle tire and the pavement surface where lateral constraint is limited [46]. In this case, a quick assessment of the initial yield point enables a rapid evaluation of the sensitivity of the asphalt concrete to viscoplastic deformation in the initial period of service life. The initial yield limit does not describe the total destruction of asphalt concrete, however, by inserting this portion of plastic deformation directly from observation, it provides additional information on the level of viscoplastic behavior in FE-based programs. It should be added that total deformation of asphalt concrete during service life does not result from reaching the state of M-C criterion. The initial yield point defines the limit stress value beyond which the viscoplastic strain may be accumulated. The value of the initial yield point is strongly related to the cohesion of the asphalt concrete and thus temperature. Accordingly, cohesion value will depend on bitumen viscosity and the level of applied load [9, 46]. By applying the stress-pseudostrains relationship, it is possible to determine the moment of obtaining the initial yield point depending on the strain rate induced. Similar analysis was performed by the authors in [9]. They also determined M-C parameters such as the internal friction angle and cohesion for the initial yield stress. These were important parameters required for complete modeling of asphalt concrete.

First, the preliminary tests were conducted according to paragraph 2.5 above – the axial compression test at a constant strain rate of 333 με/s. It can be expected that an increase in the strain rate (decrease in temperature) would result in an increase in the initial yield point, while the slowing of the strain rate (increase in temperature) in the sample would considerably decrease the initial yield limit. The result of axial compression was the average of the results obtained for two specimens. The history of the average stress-strain ratio for two asphalt concrete specimens was subjected to a smoothing process [16]. The result of asphalt concrete compression at a constant deformation rate at 40°C is shown in Fig. 6.

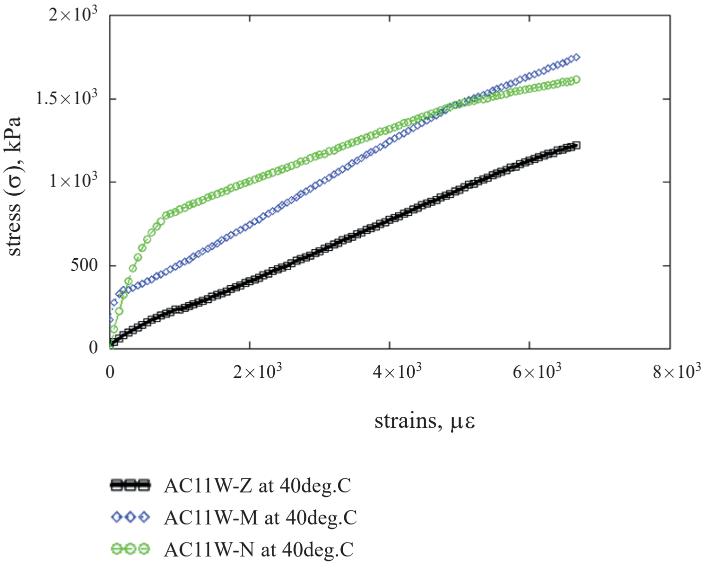

Fig. 6 Stress-strain curve in a uniaxial compressive test at 40°C

Note that at the first stage of loading the AC16W-M and AC16W-N specimens the stress increment rate as a function of deformation was low. The lowest compressive strength was demonstrated by the reference asphalt concrete, AC16W-Z. This was probably due to the presence of synthetic waxes stiffening the bitumen structure, thus increasing cohesion of the asphalt concrete. The synthetic waxes clearly defined the stress threshold, passing which leads to asphalt concrete structural damage [30] and quick strain level increase. Nevertheless, the stress-strain ratio is more favorable in asphalt concretes containing M and N types of synthetic wax.

Relationship (8) was used to estimate the pseudostrain-dependent axial stress, providing the range of stresses that were directly proportional to the pseudostrains. The $\sigma - \varepsilon_R$ relation, with the reference line representing the 1:1 ratio of stress and pseudostrains, is shown in Fig. 7.

Two regions can be distinguished in Fig. 7. The first region overlaps the equality line representing a typical asphalt concrete elastic response. Then, at a certain characteristic stress level in the given specimen, the other region is observed. In this second region, viscoplastic strains increase permanently. The sudden increase in viscoplastic strain was probably associated

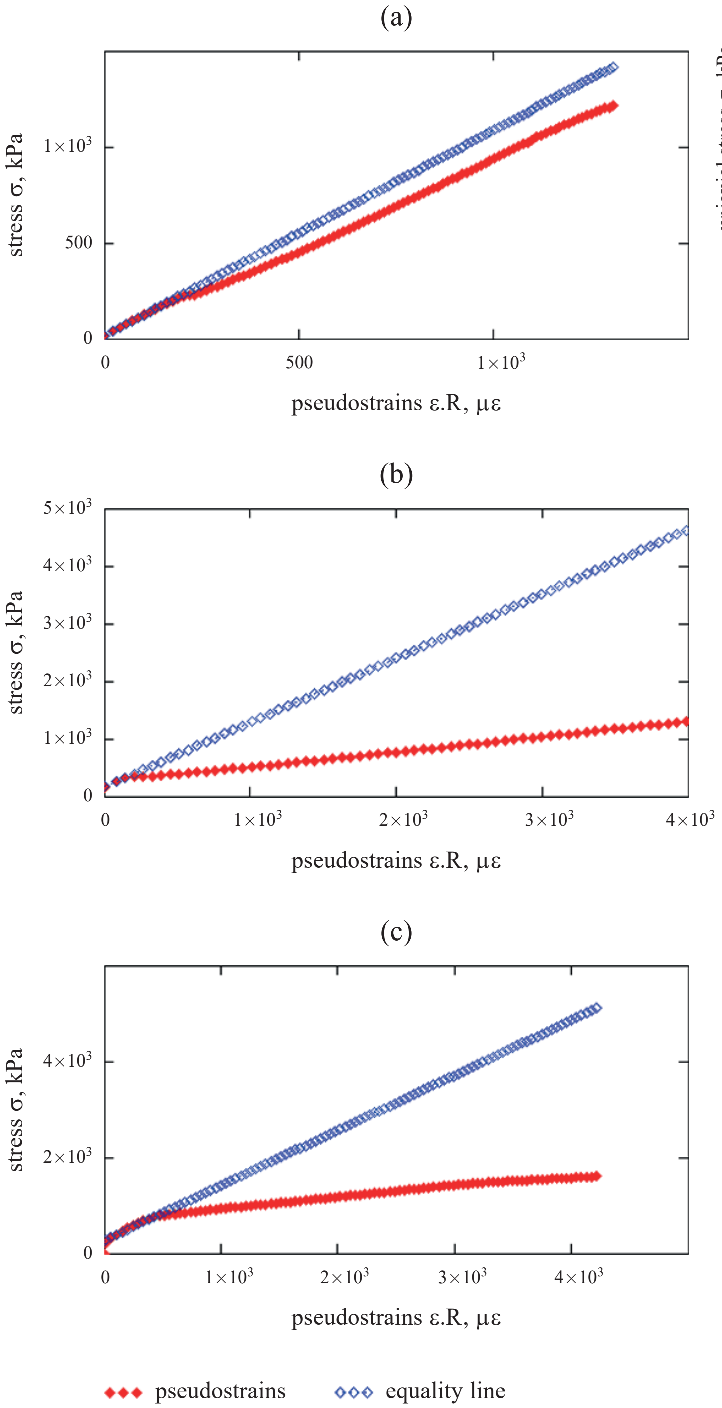

Fig. 7. Stress to pseudostrain relation at a temperature of 40°C: a) AC16W-Z; b) AC16W-M; c) AC16W-N

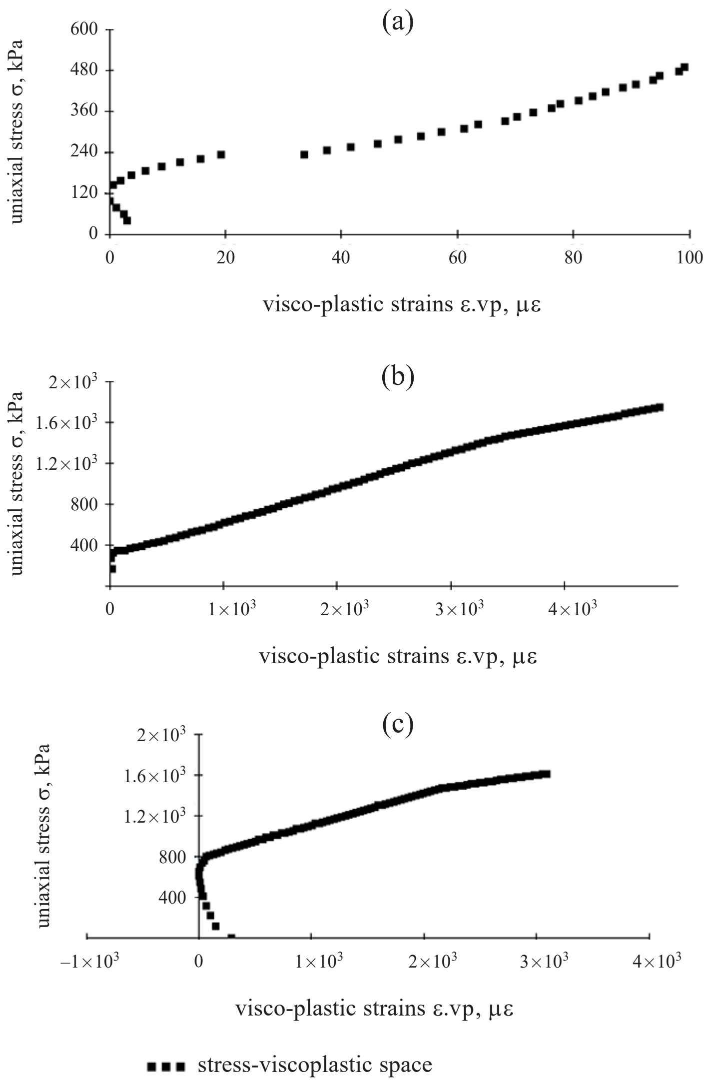

Fig. 8. Stress to viscoplastic strain relation at 40°C: a) AC16W-Z; b) AC16W-M; c) AC16W-N

with the influence of synthetic wax crystallites on the bitumen [29]. Relationship (9) was used to estimate viscoplastic strain levels, compiled with axial stress values in Fig. 8.

The change in the rate of viscoplastic response is observed in each specimen at a certain level of strain. According to the literature, this is due to aggregates interlocking in the asphalt concrete mixture at low bitumen viscosity [10]. The irregularity observed at the initial portion of the plot (Fig. 6) was probably due to the measurement device susceptibility and the effect of aggregate response at high service temperatures, observed also by other researchers [9]. The level of initial stress being the start of viscoelastic deformation, i.e. the area where the plot intersects with the axis of axial stress, is definitely the lowest in the case of reference asphalt concrete, AC16W-Z, and stands at $\sigma_{pl} = 135$ MPa. This result is consistent with the findings reported by other authors [31, 46], where the level of cohesion of asphalt concrete significantly contributed to the level of viscoplastic deformation in the near-surface area [40]. It can therefore be expected that AC16W-Z will quickly be the subject of viscoplastic deformation early in its service life. This information cannot be obtained from the elastic model parameters only. As regards AC16W-N, the stress level representing the initial yield strength is nearly 6 times higher as compared with the reference asphalt concrete, and stands at $\sigma_{pl} = 637$ MPa. For AC16W-M, $\sigma_{pl} = 316$ MPa. The initial stiffness does not necessarily indicate a high stress threshold of the yield strength. Figure 9 compiles the values of initial stiffness modulus and stress as corresponding to the initial yield strength.

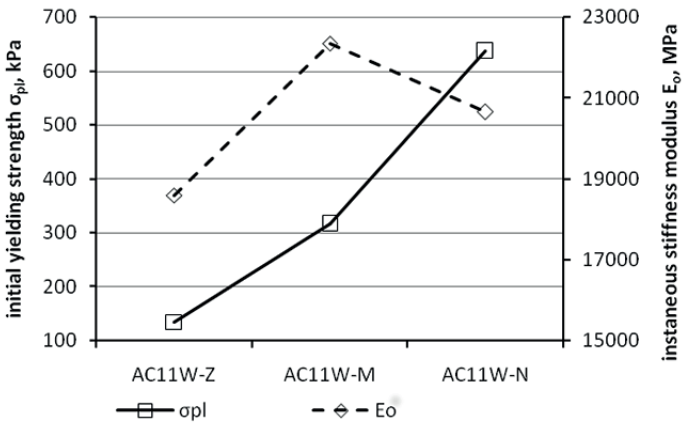

Fig. 9. Stress at which yielding begins (σ_{pl}) and stress levels of instantaneous stiffness E_o

Results of the analysis indicate that the relatively high initial stiffness is not correlated with the stress level initiating viscoplastic deformations. For example, the relatively high stiffness level of AC16W-M as compared with that of AC16W-N did not cause an increase in the limiting stress corresponding to the yield strength. This engineering practice procedure can contribute to fast approximation of yield strength level during the design of pavement structures. It will also allow for the differentiation of mixtures in terms of their susceptibility to permanent deformation and of their sensitivity to traffic induced overloading. As the tests were performed for one level of deformation rate only, it is impossible to mathematically determine the rate of deformation. Nevertheless, the data on the stress level at which asphalt concrete exhibits viscoplastic behavior and the plot of the viscoplastic strain curve can be easily introduced and used during FE modeling of pavements.

6. Conclusions

The following conclusions were drawn on the basis of the tests and analyses performed:

- the generalized Maxwell model, despite some difficulties in presenting the results in the Cole-Cole chart, has proved a good fit to the experimental data, with the mean square error below 12%,
- the highest stiffness modulus was achieved with asphalt concrete containing type M synthetic wax (AC16W-M); the lowest stiffness modulus was recorded for the reference asphalt concrete, AC16W-Z,
- the presence of type N hard synthetic waxes manifested a significant effect on the stress-strain relation,
- analysis of the stress-pseudostrain relationship allows for the registration of the stress level that initiates the formation of viscoplastic deformations,
- full description of the linear viscoelastic range of asphalt concrete requires a different deformation ratio and temperature,
- the beginning of the yield limit depends on the type of asphalt binder. Accordingly, its value depends on the strain rate in the sample and on the test temperature,
- past the initial yield strength, a sudden increase in the deviation from the reference line was observed. The characteristic stress threshold recorded during the tests increased with increasing hardness of synthetic waxes used to modify the bitumen,
- the highest yield strength, about 637 MPa, was recorded for the asphalt concrete containing type N synthetic wax (AC16W-N). This yield strength value is close to the stress generated by vehicle wheels near the surface.
- the lowest stress level corresponding to the initial yield strength was recorded for the reference asphalt concrete, AC16W-Z. This stress level suggests that the asphalt concrete will be subject to some deformation at the beginning of its service life and that it strongly depends on induced strain rate,
- the stress level of the initial yield strength was not found to directly correlate with the instantaneous stiffness modulus. Thus, under excessive loads, the pavement may experience some viscoplastic deformation,
- the stress level of the initial yield strength and corresponding viscoplastic strains can be directly applied to FE design of pavements implemented in computer software.
- The initial yield strength could be a good parameter that discerns a sensitivity of asphalt concrete to plastic deformation in the early period of service life.

References

[1] NCHRP. 2004. Contributions of Pavement Structural Layers to Rutting of Hot Mix Asphalt Pavements. Washington, D.C.: National Cooperative Highway Research Program, Transportation Research Board (TRB), National Research Council, 2002. Report 468.

[2] D.-T. Nguyen, B. Nedjar, and P.Tamagny, "Cyclic Elasto-viscoplastic Model for Asphalt Concrete Materials", *Road Materials and Pavement Design*, Volume 8, Issue 2, 2007.

[3] D.W. Christensen and R. Bonaquist R, "Use of strength tests for evaluating the rut resistance of asphalt concrete", *Association of Asphalt Paving Technologists – Proceedings of the Technical Sessions*, Vol. 71, 692–711, 2002.

[4] J.B. Sousa and S.L. Weissman, "Modeling permanent deformation of asphalt-aggregate mixes", *Journal of The Association of Asphalt Paving Technologists*, Vol. 63, 224–257, 1994.

[5] A. Zbiciak, "Mathematical description of rheological properties of asphalt-aggregate mixes", *Bull. Pol. Ac.: Tech.*, Vol. 61, No. 1, 2013, DOI: 10.2478/bpasts-2013–0005.
[6] T. Yun and Y.R. Kim. "A viscoplastic constitutive model for hot mix asphalt in compression at high confining pressure". *Construct Build Mater*, 25(5), 2733–40, 2011.
[7] L. Czarnecki and D. van Gemert, "Civil Engineering – Ongoing Technical Research. Part I", *Bull. Pol. Ac.: Tech.*, Vol. 64, No. 4, 2016 DOI: 10.1515/bpasts-2016–0075.
[8] A. Drescher, J.R. Kim, and D.E. Newcomb, "Permanent deformation in asphalt concrete", *J Mater Civ Eng*, 5(1), 112–28,1993.
[9] Y. Zhang, R. Luo, and Robert L. Lytton, "Characterization of viscoplastic yielding of asphalt concrete", *Construction and Building Materials*, Volume 47, Pages 671–679, 2013
[10] Y.R. Kim, *Modeling of Asphalt Concrete*, McGraw-Hill Construction, 2009.
[11] M. Iwański and G. Mazurek, "Optimization of the Synthetic Wax Content on Example of Bitumen 35/50" , 11th International Conference on Modern Building Materials, Structure and Techniques, MBMST, Vilnius, Lithuania, ELSEVIER, Procedia Engineering, Vol. 57, pp. 414–423, 2013, doi. 10.1016/j.proeng.2013.04.054.
[12] A. Vaitkus, D. Cygas, A. Laurinavicius, and Z. Perveneckas, "Analysis and Evaluation of Possibilities for the Use of Warm Mix Asphalt in Lithuania", *The Baltic Journal of Road and Bridge Engineering*, 4, pp. 80–86, 2009.
[13] H. Silva, J. Oliveira, J. Peralta, and S. E. Zoorob, "Optimization of warm mix asphalts using different blends of binders and synthetic paraffin wax contents", *Construction and Building Materials,* 24, 1621–1631, 2010.
[14] WT-2/2010 – *Techical requirements – Bituminous mixtures – Annex 2,* order nr 102, GDDKiA 2010.
[15] EN 12697–26 *Bituminous mixtures – Test methods for hot mix asphalt- Part 26*: Stiffness, Annex D.
[16] R. Bonaquist, "Refining the Simple Performance Tester for Use in Routine Practice", Project 9–29, *NCHRP Report 614*,Transportation Research Board, Washington, 2008.
[17] ASTM D 2166 – *Standard Test Method fo Unconfined Compressive Strength of Cohesive Soil.*
[18] P. Obara and W. Gilewski, "Dynamic stability of moderately thick beams and frames with the use of harmonic balance and perturbation methods", *Bulletin of the Polish Academy of Sciences Technical Sciences,* 64(4), pp. 739–750, 2016, doi:10.1515/bpasts-2016–0083.
[19] R.A. Schapery, "Nonlinear Viscoelastic and Viscoplastic Constitutive Equations with Growing Damage", *International Journal of Fracture*, Vol, 97, pp. 33–36, 1999.
[20] S.W. Park and R.A. Schapery, "Methods of interconversion between linear viscoelastic material functions. Part I—A numerical method based on Prony series", *Int. J. Solids Struct*. 36, 1653–1675, 1999.
[21] N.I. Yusoff, "Modelling the linear viscoelastic rheological properties of bituminous binders". *PhD thesis*, University of Nottingham, 2012.
[22] N.I. Yusoff, D. Mounierb, G. Marc-Stéphanec, M. Aireye, and H. Di Benedetto, "Modelling the rheological properties of bituminous binders using the 2S2P1D Model", *Construction and Building Materials,* 38, 2013, 395–406. doi.org/10.1016/j.conbuildmat.2012.08.038.
[23] R.A. Shapery, "Correspondance Principles and a Generalized J-integral for Large Deformation and Fracture Analysis of Viscoelastic Media", *International Journal of Fracture*, Vol. 25, pp. 195–223, 1984.
[24] E.Chailleux, G. Ramond, C.Such, and C. de La Roche, "A mathematical-based master-curve construction method applied to complex modulus of bituminous materials", *Road Materials and Pavement Design*, Volume 7, 2006.
[25] J. Judycki, P. Jaskula, M. Pszczola, J. Alenowicz, B. Dolzycki, M. Jaczewski, D. Rys, and M. Stienss, *Catalogue of typical flexible and semi-rigid pavement structures*. Gdansk University of Technology, Gdansk, Poland. (in Polish). GDDKiA (General Directorate for National Roads and Motorways), 2014.
[26] S. Mun, G.R. Chehab, and Y.R. Kim, "Determination of Time-Domain Viscoelastic Functions Using Optimized Interconversion Techniques", *Road Materials and Pavement Design*, Volume X, 2005, DOI: 10.1080/14680629.2007.9690078.
[27] Z. Pater and G. Samołyk, *Podstawy teorii i analizy obróbki plastycznej metali,* Politechnika Lubelska, Lublin, 2011, ISBN: 978–83–62596–55–327.
[28] A.A. Gonzalez, "An Experimental Study of the Deformational and Performance Characteristics of Foamed Bitumen Stabilised Pavements", *A Thesis Submitted in Partial Fulfilment of the Requirements for the Degree Pf Doctor of Philosophy in the University of Canterbury*, 2009.
[29] M. Iwański and G. Mazurek, "Structuring role of F-T synthetic wax in bitumen", *Bulletin of the Polish Academy of Sciences Technical Sciences*, Tom: 62, Zeszyt: 3, 525–534, 2014.
[30] B. Stefańczyk and P. Mieczkowski, *Mieszanki mineralno-asfaltowe. Wykonawstwo i badania*, WKŁ, Warszawa, 2008.
[31] L.A. Al-Khateeb, A. Saoud, and M.F. Al-Msouti, "Rutting Prediction of Flexible Pavements Using Finite Element Modeling", *Jordan Journal of Civil Engineering*, Vol. 5, No. 2, 173–190, 2011.
[32] A. Chomicz-Kowalska, W. Gardziejczyk, and M.M. Iwański, "Moisture resistance and compactibility of asphalt concrete produced in half-warm mix asphalt technology with foamed bitumen", *Construction and Building Materials,* 126 (2016) 108–118, doi.org/10.1016/j.conbuildmat.2016.09.004
[33] G. Mazurek, „Ocena reologicznych zmian w strukturze asfaltu spowodowanych dodatkiem wosku syntetycznego F-T", *Drogownictwo*, vol. 6, 200–204, 2015.
[34] P. Buczyński, "The Frost Resistance of Recycled Cold Mixes with Foamed Bitumen and Different Types of Road Binders", *World Multidisciplinary Civil Engineering-Architecture-Urban Planning Symposium 2016*, Procedia Engineering Volume 161, Pages 54–59, 2016, http://dx.doi.org/10.1016/j.proeng.2016.08.497
[35] D. Florea, *Nonassociated elastic viscopastic model for bituminous concrete*, Int J.Eng Sci, 32(1):87–93,1994,
[36] B.S, Underwood, Y.R. Kim, and M.N, Guddati, *Haracterization nad Performance Prediction of ALF Mixtures Using a Viscoelastoplastic Continuum Damange Model*, Journal of Association of Asphalt Paving Techologist, AAPT, Vol. 75, pp. 577–636, 2006
[37] A.C. Collop, D. Cebon, and M.S. Hardy, *Viscoelastic approach to rutting in flexible pavements*, ASCE, Journal of Transportation Eng., Vol. 121, 1995
[38] J. Judycki, P. Jaskula, M. Pszczola, J. Alenowicz, B. Dolzycki, M. Jaczewski, D. Rys, and M. Stienss, GDDKiA (General Directorate for National Roads and Motorways *), Catalogue of typical flexible and semi-rigid pavement structures*, Gdansk University of Technology, Gdansk, Poland, (in Polish), 2014.
[39] A. Drescher, J.R. Kim, and D.E. Newcomb, *Permanent deformation in asphalt concrete*. J Mater Civ Eng,5(1):112–28, 1993,
[40] J.R. Mattos, W.P. Núñez, J.A. Ceratti, A. Zíngano, and W. Fedrigo, *Shear strength of hot-mix asphalt and its relation to near-surface pavement failure – A case study in Southern Brazil*, E&E Congress 2016, dx.doi.org/10.14311/EE.2016.240

[41] P. Mackiewicz, *Parametry materiałowe mieszanek mineral-no-asfaltowych w badaniu statycznym i dynamicznym* [Material parameters of asphalt mixtures identified in static and dynamic tests], *Materiały Budowlane* 10/2015, 54–5, DOI: 10.15199/33.2015.10.16

[42] A. Zbiciak, *Identification of viscoelastic properties of bituminous mixes using classical and fractional rheological models*,Theoretical Foundations of Civil Engineering, vol. 1, Mechanics of Materials and Structures, ChapterVI, pp. 63–72, Warsaw University of Technology Publishing House, Warsaw, 2012

[43] A. Zbiciak, *Identyfication of viscoelastic properties of asphalt-aggregatemixes using classical and fractional rheological models*, XXIRUSSIAN–SLOVAK–POLISH SEMINAR, MOSCOW-ARKHANGELSK, THEORETICAL FOUNDATION OF CIVIL ENGINEERING, 2012.

[44] M.F. Woldekidan, *Response Modelling of Bitumen, Bituminous Mastic and Mortar*, PhD thesis, Faculty of Civil Engineering and Geosciences at the Delft University of Technology (TUD), 2011

[45] P. Hajikarimi, S. Mohammadi, and S. Aflaki, *Two dimensional creep analysis of linear cracked viscoelastic medium using the extended finite element method*, European Congress on Computational Methods in Applied Sciences and Engineering (ECCOMAS 2012)

[46] Near-Surface Pavement Failure Under Multiaxial Stress State in Thick Asphalt Pavement, H. Wang, and I.L. Al-Qadi, In Transportation Research Record: Journal of the Transportation Research Board, Nº 2514 TRB, National Research Council, Washington, D.C., pp. 91–99, 2010

[47] G. Mazurek and M. Iwański, *Modelling of Asphalt Concrete Stiffness in the Linear Viscoelastic Region*, Materials Science and Engineering 245 (2017) doi:10.1088/1757–899X/245/3/032029